Araque Monrós, MC.; Gamboa Martinez, TC.; Gil Santos, L.; Gironés Bernabé, S.; Monleón Pradas, M.; Más Estellés, J. (2013). New concept for a regenerative and resorbable prosthesis for tendon and ligament. Physicochemical and biological characterization of PLA-braided biomaterial. Journal of Biomedical Materials Research Part A. 101A(11):3228-3237. doi:10.1002/jbm.a.34633.

New concept for a regenerative and resorbable prosthesis for tendon and ligament. Physicochemical and biological characterization of PLA braided biomaterial.

Araque-Monrós María C.[1,2*], Gamboa-Martínez Tatiana C [1], Gil Santos Luis[1,3,5], Gironés Bernabé Sagrario[4], Monleón Pradas Manuel[1,2], Más Estellés Jorge[1].

[1]*Centro de Biomateriales e Ingeniería Tisular, Universitat Politècnica de València, 46022, Valencia, Spain*

[2]*CIBER en Bioingeniería, Biomateriales y Nanomedicina, (CIBER-BBN), Valencia, Spain*

[3]*Centro de Recuperación y Rehabilitación de Levante, (CRRL), Valencia, Spain*

[4]*Asociación de Investigación de la Industria del Textil (AITEX), Alcoy, Alicante, Spain*

[5]*Instituto Universitario de Investigación en Enfermedades Músculo-esqueléticas. Universidad Católica de Valencia (San Vicente Mártir). Spain*

**Corresponding author*

Tel: 0034 963877007 ext. 88939

Fax: 0034963877276

E-mail: marmon@upvnet.upv.es

Abstract

We present a concept for a new regenerative and resorbable prosthesis for tendon and ligament and characterize the physicomechanical and biological behavior of one of its components, a hollow braid made of poly-lactide acid (PLA) which is the load-bearing part of the prosthesis concept. The prosthesis consists of a braid, microparticles in its interior serving as cell carriers, and a surface non-adherent coating, all these parts being made of biodegradable materials. The PLA braid has a nonlinear convex stress-strain behavior with a Young modulus of 1370±90 MPa in the linear, stretched state, and after 12 months of hydrolytic degradation the modulus shows a reduction by a factor of four. Different disinfection methods were tested as to their efficiency in cleansing the braid and preparing it for cell culture. Fibroblasts of L929 line were grown on the PLA braid for 14 days, showing good adherence and proliferation. These studies validate the PLA braid for the intended purpose in the regenerative prosthesis concept.

Keywords: prosthesis, tendon, ligament, resorbable, regenerative

1. Introduction

Both tendons and ligaments are highly specialized and evolved connective tissues; tendons have a double mechanical task: to transfer movement from muscles to bones, and to withstand the forces originating in those movements. Ligaments join bones to bones and stabilize the joints, resisting and transferring the forces generated in such movements. Excessive forces and trauma damage the tissues affecting their function and mobility.[1,2] Most of tendon and ligament injuries come from daily activity like practicing sports or labor accidents, but they may be also due to degenerative pathologies or tumors. On the whole, injuries in tendons and ligaments are among the most frequent pathologies affecting the adult population, which disturb the quality of life and result in a high economic cost.[3,4] Thus, a clear need to improve patient situation exists, and has been addressed in the course of time with different concepts. Alongside the prolonged experience with a variety of autografts or allografts,[5] biological[6-8] or synthetic[9-11] prostheses, the new possibilities opened by cell therapy lead current research in the direction of not just restoring the mobility and functionality of the patient but also of developing new therapies able to regenerate the damaged biological tissue and restore the biomechanical strength of tendons and ligaments. Stem cells from bone marrow, which are multipotent cells with a high differentiation potential to tenocytes have been proposed with this purpose[12,13] Growth factors improve the repair tissue,[14] enhance the expression of type I and III collagen,[15,16] improve the cellular proliferation,[17,18] and promotes the healing process[19,20]; gene therapy strategies have been also tried[21,22]. Tissue engineering makes use also of synthetic scaffolds for tendon and ligament regeneration. Braids made from PLA and poly-glycolic acid (PGA) are some of the most commonly used structures due to their morphological and mechanical properties. PLA and PGA can be used separately or copolymerized.[23] Both materials have been approved by the FDA for many uses in humans, have shown a good biological response, and their mechanical properties can be tailored through the

braiding features.[23-27] They are both resorbable materials degrading hydrolytically without any damage to the body. These materials have a slow degradation in vivo, and several years pass until they completely disappear; nevertheless, in vitro lower molecular weight products and a loss of mechanical properties in the early months of degradation are obtained.[28-31]

Our concept of a "regenerative prosthesis"[32] tries to combine into a single construct the load bearing and replacement functions usually covered by a traditional prosthesis with the ability to regenerate the lost tissue and progressively be replaced by it. Since tendons and ligaments need immediate mobility to avoid adherences and load-bearing capacity after any repair strategy, a pure cell-based strategy is unlikely to succeed in the case of important lesions or degeneracies. Thus, at a first healing stage, the features of a traditional prosthesis are needed, guaranteeing immediate mobility and resistance. The load transfer to progenitor cells thus ensured may trigger the guided regeneration of the neotissue. With this hypothesis in mind, we combine a resisting braid which has a hollow interior and contains a progenitor cell supply in this space. The cells are thus protected and kept in place more efficiently than in the case they were seeded on top of the construct. The cell supply is vehicled by microparticles acting as cell carriers and as a three-dimensional scaffold. Finally, in order to avoid undesired tissue adherences, the exterior of the braid is coated by a non-adherent hyaluronic acid film. All the construct's components are biodegradable, and should be completely resorbed in the course of time. In order to adapt the prosthesis concept to specific tendons or ligaments the dimensions of the braid and the braid characteristics (number of threads, braiding angle) should be adjusted. In this paper we characterize a nonspecific in this sense PLA hollow braid; we investigate its mechanical properties, its in vitro degradation, and its biological performance in vitro with a fibroblasts cell line.

2. Materials and methods

2.1 PLA braid

PLA microfibers (Ingeo, Natureworks PLA Polymer 6251D), with a linear density of 0,22 tex (1 tex=1 g/1000 m), made from poly-L-lactide PLLA, blended with 1,4 % of poly-D-lactide PDLA, were used to manufacture a hollow cylindrical (tubular) braid using a braiding machine Herzog NG 2/12-120 (Oldenburg, Germany). The braid was made with 12 threads, each of them made with 4 sets of 150 microfibers (7200 microfibers altogether). The linear density of the resulting braid was 1612,8 tex. The microfibers were braided around a PLA thread of 330 tex, subsequently removed to obtain the tubular shaped braid. Both the cross section of microfibers and an effective cross section of the braid were computed from their linear mass densities (M/L), given in tex, through equation (1):

$$S=\frac{V}{L}=\frac{M}{L\rho_{PLA}} \quad (1)$$

Density of PLA was taken from data sheet of manufacturer ρ_{PLA}= 1.24 g/ml.[33]

2.2 Morphology

The physical appearance of the braid was observed with an optical microscope (Leica MZ APO, Germany) and a scanning electronic microscope (SEM) JEOL JSM-5410 working at 10 kV. Previously to SEM the samples were coated with a thin gold layer using the sputtering technique. Inner and outer diameter of braid, braid angle and diameter of microfibers were measured from pictures (n=3) and were calculated the average.

2.3 Tensile properties

The mechanical properties of the PLA braid were characterized with two different mechanical tests: stress-strain and dynamic test. Both tests were carried out on a stress-strain test machine (MICROTEST SCM 4000 98, Spain) with a load cell with range up to 400 N. Measurements were performed at room temperature by triplicate.

Stress-strain tests of the complete braid and of four unbraided threads simultaneously, each thread made out of 4 sets of 150 microfibers (600 microfibers altogether), were performed at a 5 mm/min stretching rate, recording the values of load and deformation each second. The Young modulus was computed from the slope of the linear region of measured curve, according to the equation (2):

$$E = \frac{\sigma}{\varepsilon} = \frac{F/S}{\Delta l/l} \qquad (2),$$

where F is the applied load, S the effective cross section of the sample, l the length and Δl the deformation of sample. Both the cross section of microfibers and the effective cross section of braid were computed through equation (1).

The limit of the "toe" region of the deformation curve, which corresponds to the lower deformation, nonlinear part of the curve before the linear behaviour, was defined as the deformation at which the tangent line drawn to the linear part of the curve separates from the curve. The limit of linearity (σ_{lim}) was taken as the highest stress where the linear behavior of curve ceased.

Braids as received and after different degradation times were subjected to stress-strain assays of the type described above until failure, in order to determine the breaking load and the elongation (%).

The dynamic tests on the braids were performed selecting values of applied force to ensure deformations within the linear region of the material, between 30N-90N. A stretching was applied at 5 mm/min until 60 N load and 100 subsequent sinusoidal load cycles of amplitude 30 N at a frequency of 0.5 Hz were superposed. 5 out of 10 cycles were recorded (20 data/s). The lost energy per unit of volume in each cycle was computed from the area of mechanical hysteresis cycle due to the phase lag between stress and strain, through equation (3):

$$\%\, Hysteresis = \frac{W_c}{W_T} \cdot 100 \qquad (3)$$

where W_c is the enclosed surface area in the hysteresis cycle and W_T is the enclosed area between the loading curve and the strain axis. Given data are averaged from three tested samples.

2.4 Differential scanning calorimetry (DSC)

Differential scanning calorimetric measurement of braid was carried out in a calorimeter (METTLER TOLEDO, DSC 823e, Switzerland) using nitrogen as purge gas (20 ml/min). The temperature of the equipment was calibrated with Indium, and the melting enthalpy of Indium was used to calibrate the heat flux. One heating scan was evaluated. Measurement was performed from 0°C to 210°C at 10°C/min. The weight of the tested sample ranged between 5 and 10 mg. Different parameters were determined from the thermogram: the glass transition temperature, Tg, the melting temperature, Tm, the melting crystallization, ΔHc and the melting enthalpy, ΔHm. The crystallinity of the PLA braided material (*Xc*) was determined according to equation 4, making use of the reported melting enthalpy of PLA crystals, $\Delta H^{o}_{PLA} = 93.7$ J/g.[34]

$$X_c = \frac{\Delta H_m}{\Delta H_m^o} x100\% \quad (4)$$

2.5 Degradation assay

Hydrolytic degradation of the hollow PLA braid in Dulbecco's phosphate-buffered saline, DPBS (Sigma) (pH=7.4) with 0.2 mg/ml of sodium azide 99% (Aldrich), at 37°C along 12 months was studied. Before the degradation process, the mass of each sample was measured (m_0) with an analytical balance (XS Excellence, USA). The medium was changed weekly but previously its pH was measured using a pH-meter (Eutech Instruments model PH1500, Singapore), in order to verify the pH was stable at pH=7.4. After each degradation time, a set of samples (n=3) was taken out, washed with distilled water at 50ºC and finally dried in vacuum at 37 ºC until constant weight. Washing with distilled water was done in order not to affect the properties of the material and to remove any salt that could have been deposited on the surface of the material. The mass of each sample was measured (m_d) and the weight loss was computed according to equation (5).

$$\text{Weight loss } \% = \frac{(m_0 - m_d)}{m_0} \times 100 \quad (5)$$

The mechanical properties of samples degraded for 2, 4 and 12 months were determined as explained above, also by triplicate. In these degraded samples the Young modulus, the limit of linearity (σ_{lim}), the breaking load and the elongation (%) were determined.

2.6 Cytotoxicity assays to select the best sterilization methodology

Cytotoxicity test of the hollow braids sterilized with different methods was carried out following the standard UNE-EN ISO10993-5 norm by the indirect method. Briefly, the test was based on the study of viability of cells in a culture medium that had been previously in contact with the material for 24h at 37°C and constant shaking, 60 rpm, in sterile conditions. Pieces of PLA braids were subjected to different sterilization methods: 1) immersion in aqueous ethanol solution at 70% concentration, (EtOH 70%) for 4h with changes every 30 min, 2) exposure to a 30 W

ultraviolet irradiation (UV) overnight, and 3) autoclave (Mocom Proxima, Germany) for 30 min at 120ºC. Mouse fibroblasts L929 cell line (Sigma, Spain) was employed for the cytotoxicity test. Latex was used as positive control material and an empty well of the culture plate was used as negative control. Strictly speaking, method (1) above (70% ethanol solution) is not a sterilization method, but a disinfectation method; it was, nonetheless, compared with the other two sterilization methods in order to choose the methodology of the study.

In order to get the extracts, 1 g of braid and 1 g of latex were incubated separately in 20 ml of Dulbecco's modified eagle medium, DMEM (Sigma) 1 g/l D-glucose, supplemented with 10% of fetal bovine serum, FBS (Fisher), 1% penicillin/streptomycin, 1% L-glutamine (Lonza) , for 24 h at 37°C at 60 rpm. Subsequently, 3.500 cells/well were seeded on a 48-well culture plate; after 24 h of culture the medium was replaced by the extracts: in the case of the positive control, medium incubated with latex; in the case of the negative control, normal medium. Afterwards, plates were incubated at 37°C and 5% CO_2, keeping the extract as culture medium for the 14 days of the test duration. Samples were taken out at 1, 3, 7 and 14 days.

2.7 Cell culture

Hollow PLA braids of 8 mm length were disinfected with EtOH 70% before culture. L929 cells in passage 8 were used. Cells were cultured in 75 cm^2 flask using DMEM (Sigma) 4.5 g/l D-glucose, with 10% of FBS, 1% penicillin/streptomycin, 1% L-glutamine until confluence, then they were enzymatically detached with 5 ml of trypsin (Sigma) and counted with a hemocytometer (Labor Optik, China). Subsequently, 50 µl of a cellular suspension (11.000 cells) were seeded on the surface of each PLA braid. Samples were incubated for 1 h at 37°C and 5% CO_2 to promote adhesion and afterwards culture medium was added. The culture plate was used as control material. Medium was replaced every three days. Testing times were 1, 7 and 14 days.

2.8 Cell viability

Cellular viability was assessed using 3-(4,5-dimethylthiazol-2-yl)- 5-(3-carboxymethoxyphenyl)-2-(4-sulfophenyl)-2H-tetrazolium), with the Cell Titer 96 Aqueous One Solution Cell Proliferation Assay, MTS (Promega). After different culture times (1, 7 and 14 days), samples were placed on a 48-well culture plate and washed with DPBS. Culture medium, DMEM (without phenol red and without FBS) was mixed with the MTS reagent (5:1) and 300 µl were added to each well and incubated at 37°C and 5% of CO_2 without light. After three hours 100 µl of medium were taken out and placed in 96-well culture plate wells to measure the absorbance at 490 nm using a multiplate reader (Victor 3, PerkinElmer, USA). The test was performed in triplicate (n=3).

2.9 Cell adhesion and morphology

Morphology and adhesion of cells were analyzed using SEM, JEOL JSM-5410 at 10 kV. After culture times, the samples were washed in DPBS, fixed with glutaraldehyde 2.5% solution (Electron Microscopy Science) for 1 h at 4ºC and washed with DPBS. Samples were dehydrated washing with several ethanol-water solutions with increasing ethanol concentration until 100% concentration. Samples were critical-point dried and covered with gold for further analysis.

2.10 Fluorescence analysis

Distribution and cell adhesion were assessed staining the actin cytoskeleton of cells and using a confocal scanning microscopy with inverted laser (Leica TCS SP2 AOBS, Germany). Samples were washed with PB 0.1 M (sodium di-hydrogen phosphate 2-hydrate and disodium hydrogen phosphate anhydrous solved in water 1:4) for 5 minutes at room temperature. A buffer blocking

solution (TB) containing 8,9 mL of PB (0,1 M), 1 mL of FBS and 0,1 mL of triton X-100 was added for 2 h at room temperature; TB with 10µl/sample of bodipy-FL phallacidin (Invitrogen) was added to each sample until they were completely covered and remained over night at 4ºC without light. Next morning, solution was removed and samples were washed three times with PB 0.1 M every 5 minutes. Finally, samples were placed on microscope slide adding a drop of Vectashield with incorporated 4',6-diamidino-2-phenylindole, DAPI (Vector Laboratories, Peterborough, UK) in order to dye the nuclei.

2.11 Statistical analysis

Statistical analysis was done with the *t Student* test, using SPSS 16.0 and a significance value of $p<0.05$.

3. Results

3.1 Morphological characteristics of the braids

The morphology of the hollow PLA braid can be seen in Figure 1, where the overall appearance and the relevant details of braiding angle and dimensions can be seen. The braid is formed by twelve multifilament threads, each about 500 microns (Figure 1c), each thread being composed by four sets of 150 monofilaments (single fibers), Figure 1d. The inner and outer diameters of the braid were 1,9±0,2 mm and 0,9±0,03 mm. The braiding angle was 80±7º. The observed diameter of the single microfibers was 15±0,5 µm. From the linear density given by the manufacturer, 0,22 tex a computed microfiber diameter can be obtained as: $\Phi = \sqrt{\frac{4 \cdot 10^{-6} \cdot dtex}{\pi \rho_{PLA}}}$. The observed and the computed diameters are thus in good agreement.

3.2 Tensile properties

Figure 2 plots the stress-strain behavior of PLA threads and of the PLA braid. The threads exhibit a linear behavior, while the braid characteristic is nonlinear. The Young modulus of microfibers was 5120±150 MPa. When load is applied to the braid, the threads start to align in the same direction of the applied load, increasing the deformation with only small loads, giving the first deformation region of small but increasing modulus, the so-called "toe" region; the limit of this region was $\varepsilon_{toe,}$ 3±0,1 %. With progressive orientation of the threads in the direction of load the braid becomes stiffer due to the stretch of an increasing number of threads, until all of them are stretched and a linear deformation region is attained. The linear modulus in this region is 1370±90 MPa. Linear behavior is lost for load values greater than σ_{lim}=77.5±0.7 MPa; from this point, if load was increased, the Young modulus decreased. Thus the stress–strain behavior of the braid is similar to that of ligament and tendon.[27,35]

When stretched cyclically under equal load cycles the braid shows an increase of non-recoverable deformation (Figure 3a), of the order of a 7% strain after 90 cycles. The percentage of mechanical hysteresis, which is an indication of the relative loss of energy in each cycle, shows a decreasing tendency, and stabilizes around 9 % after cycle 50. This energy loss must be attributed both to the viscoelasticity of the material and to the friction among the microfibers while they orient.

3.3 Differential scanning calorimetry (DSC)

As a way to assess the chemical quality of the PLA employed by the manufacturer to produce the braid a DSC analysis was undertaken of pieces of the braid. Figure 4 shows the thermogram obtained during the heating scan of the material as received. At room temperature the material is in the glassy state, below its Tg; the glass transition occurs at approximately 62ºC; immediately

above this temperature range an exothermal peak is clearly manifest on the curve, due to the crystallization of chains which were previously metastably trapped in the glassy state, and now acquire enough mobility to reaccomodate and crystallize. At still higher temperatures the material finally melts, and the thermogram exhibits the typical melting endothermal peak. From this curve values of the glass transition temperature, the melting temperature and the crystallization and melting enthalpies could be obtained by standard procedures. A comparison of the melting enthalpy with the melting enthalpy of a single PLA crystal allows to obtain the degree of crystallinity (crystalline phase mass fraction) of the material; in order to determine the value of this quantity for the material as received (room temperature), the crystallization enthalphy was subtracted from the melting enthalpy and the result divided by the single-crystal melting enthalpy value. All these quantities are given in Table 1; they agree with values for PLA reported in the literature.[36] Since the computed Tg of the material lies some 25 degrees above body temperature, processes occurring in the glassy state can be safely assumed to be absent or taking place at a very slow pace; thus PLA can be regarded as a physically stable material at body temperature.

3.4 Hydrolytic degradation of the braid

When kept in PBS at constant pH of 7.4 pieces of the PLA braid show a negligible loss of weight after two months (Figure 5); according to Student's *t* test, the change of weight is not statistically significant after that period. The approximately 1% mass fraction loss after 12 months of degradation test occurs during the first two months. Young modulus, breaking load, elongation (%) and limit of linearity (σ_{lim}) of degraded braids were determined after different degradation times and can be seen on Table 2. The effects of the hydrolytical chain scission can be clearly appreciated in the steady decrease of the material's breaking strength and Young modulus. However, these changes are not accompanied by a significant loss of weight. This suggests that

the chain fragmentation due to hydrolysis produces low molecular weight chain fragments that remain trapped somehow inside the structure, probably entangled in a way that impedes their diffusion through the bulk of the material.

3.5 Cytotoxicity of the material

In order to select a disinfectation method cellular viability was evaluated qualitatively with the optical microscope (Figure 6) and quantitatively with a MTS assay (Figure 7). Cells cultured using the positive cytotoxic control (latex) and the supernatant of the braid sterilized with UV extract showed a rounded shape, indicating cell death. Cells cultured in the supernatant medium of braids disinfected with EtOH 70% showed the stretched morphology which is usually seen in fibroblasts, very similar to that observed on negative (non cytotoxic) control, which indicates a suitable proliferation. These qualitative findings are corroborated quantitatively on Figure 7. Cells in contact with latex were non-viable from the first day, suggesting that this material is toxic for cells. Cells cultured with extract of both braid sterilized with UV and with autoclave showed signs of cytotoxicity from the seventh day. This may be due to the thickness of the PLA braid and the large quantity of microfibers, which may impede UV radiation to penetrate the entire volume of the braid. In addition, materials sterilized with autoclave became stiffer because the high temperatures reached during sterilization process imply a further crystallization of the PLA (see the DSC results). By contrast, cells cultured in extract of PLA braid disinfected with EtOH 70% did not show toxic effects, although the viability at 14 days is lower than in the negative control. These results validated the choice of, EtOH 70% as a more effective disinfectation technique than the alternatives studied.

3.6 Cell Viability, Adhesion and Morphology on Braids

When seeded on the braids and cultured, the number of viable cells increased with time, as revealed by the MTS assay (Figure 8). Morphology and cellular adhesion of L929 fibroblasts can be seen on Figure 9. Morphology of fibroblasts changed with the course of time from a rounded shape observed in the first day to a stretched shape seen from the seventh day on. The cells were elongated in the direction of fibers, and after 14 days the fibres were completely coated by cells. The cytoplasm spread revealed by the micrographs is indicative of a good cell adhesion on the PLA microfibres through cytoplasmic extensions. Staining of the actin cytoskeleton and cellular nuclei gives additional information of the cell adhesion and spread on the fibers (Figure 10). Cells exibited rounded shape after the first day of culture; for higher culture times, cells showed a stretched morphology with a cytoskeleton well developed and well defined nuclei. After 14 days of culture was observed a green staining completely covering the braided material Actin is a cytoskeleton protein that provides scaffolding to the cell; it self-reorganizes depending on the cell's envirenment characteristics and makes up the necessary microfilaments for cell migration. The well-developed actin cytoskeleton assessed by fluorescence indicates that on our braids the cells adhered well and were able to migrate and colonize the length of the filaments.

4. Discussion

Tissue engineering of tendon and ligament tries to overcome the limitations encountered in the regeneration of the damaged biological tissue by combining the pluripotency of some cell lineages with material scaffolds.[37] The concept of a regenerative tendon prosthesis here envisaged relies on the capability of supplied cells to regenerate a neotissue when properly stimulated mechanically and biochemically *in situ*. A PLA hollow braid can fulfill two missions in this

strategy: to provide the necessary *in vivo* initial strength and transmit the mechanical loads to the cells in its interior, and to protect this cell supply while differentiation and ulterior regeneration takes place *in vivo*. For these reasons, a first step in this direction was to characterize both the mechanical and the biological behavior of PLA braids. Tendons and ligaments usually work in toe region and in the first part of the linear region,[38] where tendon has values of the Young modulus of about 1-2 GPa,[39] ligaments show values between 0,5-1 GPa.[40] The stress-strain curve of our PLA braids show a nonlinearly convex characteristic with an initial "toe" region followed by a developed linear behavior with a Young modulus of 1.4 ± 0.9 GPa, similar to that of tendons. Further, the linear region extended up to stresses about $\sigma_{lim} = 77 \pm 0.7$ MPa, higher than the limit estimated for tendons and ligaments, reported to be about 30 MPa.[41] In order to match the higher linear moduli of ligaments one may intervene on the features of braiding.[27,41] In addition, the estimated mechanical hysteresis of the braids (9%) was in the range of reported values for tendon, between 3% and 38%.[42,43] This property is of functional importance for the dynamic behaviour of tendons and ligaments, bearing a relation to the amount of metabolic energy that can be saved during locomotion[42]. These results validate the intended use of the PLA braids from the point of view of their initial, post-implantation immediate mechanical behaviour.

The prosthesis must progressively be resorbed *in vivo* while the neotissue grows. We undertook the characterization of the *in vitro* degradation of the braided PLA by following in time the loss of mass and of mechanical strength and modulus. The remarkable absence of significant mass loss after 12 months of hydrolytic degradation contrasts with the noteworthy change of the mechanical properties in that time. This suggests that the PLA is hydrolytically degraded but the smaller chain fragments resulting become entangled with other chains and do not diffuse easily outside the material, remain trapped in the bulk, and do not give rise to an appreciable weight loss. Nevertheless, the hydrolysis of the ester bonds of the amorphous phase of PLA is reflected

in the loss of mechanical properties when degradation proceeds.[44,45] The complete degradation of PLA braid in the body may take a time which is difficult to estimate when speaking about tendons and ligaments; it may take several years as surgical experience in other tissues shows.[46]

The characterization of the cell-braid interaction *in vitro* also supports the intended use of the braid. The material could be shown to be devoid of cytotoxic effects after being disinfected with a 70% aqueous ethanol solution.[47] This method was more efficient than alternative sterilization methods, probably because the multistranded morphology of the braid results in places inaccessible for radiation. Autoclave couldn't be used with PLA since it modifies the physical state of the material. Thus treated, the PLA braids are a good support for the growth of fibroblasts seeded on the surfaces of the threads. Staining of the nuclei and of the actin cytoskeleton revealed that these cells proliferated and adhered on the braids, and completely covered the available surface after 14 days. These results agree with previous studies on braided PLA.[5]

Our study of the cell-material interaction with the L929 cell line *in vitro* is intended as a model study. Clinical translation of the concept will involve instead some kind of mesenchymal stem cells. For obvious reasons, adult autologous cells seem those more probable to enter a clinical solution. The use of differentiated tenocytes is discouraged by different researchers because these cells lose their phenotype during prolonged monolayer culture; furthermore these cells are present in low density and their extraction could cause zonal damage. Bone marrow mesenchymal stem cells (BM MSCs) and adipose tissue-derived stem cells (ADSC) have been successfully differentiated to functional tenocyte-like cell,[48-50] so these cells are best candidates to try the regeneration of the tendon and ligament. *In vivo* tests with these cells using small animals are planned as a next step in order to validate the hypothesis of our prosthesis concept.

Acknowledgements

This work has been developed thanks to the financial support of AITEX (Valencia, Spain). JME thanks Drs. Isabel Pascual, Andrés Peña and their team from Hospital Clínico of Valencia for their fine work.

References

1. Vieira AC, Guedes RM, Marques AT. Development of ligament tissue biodegradable devices: A review. Journal of Biomechanics 2009;42(15):2421-2430.
2. Kuo C, Marturano J, Tuan R. Novel strategies in tendon and ligament tissue engineering: Advanced biomaterials and regeneration motifs. Sports Medicine, Arthroscopy, Rehabilitation, Therapy & Technology 2010;2(1):20.
3. Butler DL, Juncosa-Melvin N, Boivin GP, Galloway MT, Shearn JT, Gooch C, Awad H. Functional tissue engineering for tendon repair: A multidisciplinary strategy using mesenchymal stem cells, bioscaffolds, and mechanical stimulation. Journal of Orthopaedic Research 2008;26(1):1-9.
4. Deborah P L. The costs of musculoskeletal disease: health needs assessment and health economics. Best Practice & Research Clinical Rheumatology 2003;17(3):529-539.
5. Cooper JJA, Bailey LO, Carter JN, Castiglioni CE, Kofron MD, Ko FK, Laurencin CT. Evaluation of the anterior cruciate ligament, medial collateral ligament, achilles tendon and patellar tendon as cell sources for tissue-engineered ligament. Biomaterials 2006;27(13):2747-2754.
6. Zheng MH, Chen J, Kirilak Y, Willers C, Xu J, Wood D. Porcine small intestine submucosa (SIS) is not an acellular collagenous matrix and contains porcine DNA: Possible implications in human implantation. Journal of Biomedical Materials Research Part B: Applied Biomaterials 2005;73B(1):61-67.
7. Daniel K L. Achilles tendon repair with acellular tissue graft augmentation in neglected ruptures. The Journal of Foot and Ankle Surgery 2007;46(6):451-455.
8. Seldes RM, Abramchayev I. Arthroscopic insertion of a biologic rotator cuff tissue augmentation after rotator cuff repair. The Journal of Arthroscopic and Related Surgery 2006;22(1):113-116.
9. Miller MD, Peters CL, Allen B. Early aseptic loosening of a total knee arthroplasty due to Gore-Tex particle-induced osteolysis. The Journal of Arthroplasty 2006;21(5):765-770.
10. Dominkus M, Sabeti M, Toma C, Abdolvahab F, Trieb K, Kotz RI. Reconstructing the extensor apparatus with a new polyester ligament. Clinical orthopaedics and related research 2006;453:328-334
11. Murray AW, Macnicol MF. 10 -16 year results of Leeds-Keio anterior cruciate ligament reconstruction. The Knee 2004;11(1):9-14.
12. Krampera M, Pizzolo G, Aprili G, Franchini M. Mesenchymal stem cells for bone, cartilage, tendon and skeletal muscle repair. Bone 2006;39(4):678-683.
13. Caplan AI. Review: mesenchymal stem cells: cell-based reconstructive therapy in orthopedics. Tissue engineering 2005;11(7-8):1198-211.
14. Kimura Y, Hokugo A, Takamoto T, Tabata Y, Kurosawa H. Regeneration of anterior cruciate ligament by biodegradable scaffold combined with local controlled release of basic fibroblast growth factor and collagen wrapping. Tissue Engineering Part C-Methods 2008;14(1):47-57.
15. Wei XL, Lin L, Hou Y, Fu X, Zhang JY, Mao ZB, Yu CL. Construction of recombinant adenovirus co-expression vector carrying the human transforming growth factor-beta1 and vascular endothelial growth factor genes and its effect on anterior cruciate ligament fibroblasts. Chinese medical journal 2008;121(15):1426-32.

16. Spindler KP, Murray MM, Detwiler KB, Tarter JT, Dawson JM, Nanney LB, Davidson JM. The biomechanical response to doses of TGF-β2 in the healing rabbit medial collateral ligament. Journal of Orthopaedic Research 2003;21(2):245-249.
17. Kurtz CA, Loebig TG, Anderson DD, DeMeo PJ, Campbell PG. Insulin-like growth factor I accelerates functional recovery from Achilles tendon injury in a rat model. The American journal of sports medicine 1999;27(3):363-9.
18. Dahlgren LA, van der Meulen MCH, Bertram JEA, Starrak GS, Nixon AJ. Insulin-like growth factor-I improves cellular and molecular aspects of healing in a collagenase-induced model of flexor tendinitis. Journal of Orthopaedic Research 2002;20(5):910-919.
19. Molloy T, Wang Y, Murrell GAC. The roles of growth factors in tendon and ligament healing. Sports Medicine 2003;33(5):381-394.
20. Costa MA, Wu C, Pham BV, Chong AKS, Pham HM, Chang J. Tissue engineering of flexor tendons: Optimization of tenocyte proliferation using growth factor supplementation. Tissue Engineering 2006;12(7):1937-1943.
21. Jayankura M, Boggione C, Frisén C, Boyer O, Fouret P, Saillant G, Klatzmann D. In situ gene transfer into animal tendons by injection of naked DNA and electrotransfer. The Journal of Gene Medicine 2003;5(7):618-624.
22. Huang D, Balian G, Chhabra AB. Tendon tissue engineering and gene transfer: The future of surgical treatment. The Journal of Hand Surgery 2006;31(5):693-704.
23. Lu HH, Cooper JA, Manuel S, Freeman JW, Attawia MA, Ko FK, Laurencin CT. Anterior cruciate ligament regeneration using braided biodegradable scaffolds: in vitro optimization studies. Biomaterials 2005;26(23):4805-4816.
24. Laurencin CT, Freeman JW. Ligament tissue engineering: An evolutionary materials science approach. Biomaterials 2005;26(36):7530-7536.
25. Deng D, Liu W, Xu F, Yang Y, Zhou G, Zhang WJ, Cui L, Cao Y. Engineering human neo-tendon tissue in vitro with human dermal fibroblasts under static mechanical strain. Biomaterials 2009;30(35):6724-6730.
26. Eijk FV, Saris DBF, Riesle J, Willems WJ, Blitterswijk CAV, Verbout AJ, Dhert WJA. Tissue engineering of ligaments: A comparison of bone marrow stromal cells, anterior cruciate ligament, and skin fibroblasts as cell source. Tissue Engineering 2004;10:5/6.
27. Freeman JW, Woods MD, Laurencin CT. Tissue engineering of the anterior cruciate ligament using a braid-twist scaffold design. Journal of Biomechanics 2007;40(9):2029-2036.
28. Loo SCJ, Tan HT, Ooi CP, Boey YCF. Hydrolytic degradation of electron beam irradiated high molecular weight and non-irradiated moderate molecular weight PLLA. Acta Biomaterialia 2006;2(3):287-296.
29. Saha SK, Tsuji H. Effects of molecular weight and small amounts of d-lactide units on hydrolytic degradation of poly(l-lactic acid)s. Polymer Degradation and Stability 2006;91(8):1665-1673.
30. Iannace S, Maffezzoli A, Leo G, Nicolais L. Influence of crystal and amorphous phase morphology on hydrolytic degradation of PLLA subjected to different processing conditions. Polymer 2001;42(8):3799-3807.
31. Tsuji H, Ikarashi K, Fukuda N. Poly(l-lactide): XII. Formation, growth, and morphology of crystalline residues as extended-chain crystallites through hydrolysis of poly(l-lactide) films in phosphate-buffered solution. Polymer Degradation and Stability 2004;84(3):515-523.

32. Araque Monros MC., Mas Estelles J., Monleón Pradas M., Gil Santos L., S. GB. Process for obtaining a biodegradable prosthesis. P201130913 2011.
33. Garlotta D. A Literature Review of Poly(Lactic Acid). Journal of Polymers and the Environment 2001;9(2):63-84.
34. Tsuji H, Ikada Y. Properties and morphologies of poly(l-lactide): 1. Annealing condition effects on properties and morphologies of poly(l-lactide). Polymer 1995;36(14):2709-2716.
35. Hooley CJ, McCrum NG, Cohen RE. The viscoelastic deformation of tendon. Journal of Biomechanics 1980;13(6):521-528.
36. Quynh TM, Mitomo H, Nagasawa N, Wada Y, Yoshii F, Tamada M. Properties of crosslinked polylactides (PLLA & PDLA) by radiation and its biodegradability. European Polymer Journal 2007;43(5):1779-1785.
37. Chen J, Xu J, Wang A, Zheng M. Scaffolds for tendon and ligament repair: review of the efficacy of commercial products. Expert Review of Medical Devices 2008;6(1):61-73.
38. Johnson GA, Tramaglini DM, Levine RE, Ohno K, Choi N-Y, L-Y. Woo S. Tensile and viscoelastic properties of human patellar tendon. Journal of Orthopaedic Research 1994;12(6):796-803.
39. Maganaris CN, Narici MV, Reeves ND. In vivo human tendon mechanical properties: effect of resistance training in old age. J Musculoskel Neuron Interact 2004;4(2):204-208.
40. Rees JS, Jacobsen PH. Elastic modulus of the periodontal ligament. Biomaterials 1997;18(14):995-999.
41. Magnusson SP, Aagaard P, Rosager S, Dyhre-Poulsen P, Kjaer M. Load displacement properties of the human triceps surae aponeurosis in vivo. Journal of Physiology 2001;531(1):277-288.
42. Maganaris CN, Paul JP. Tensile properties of the in vivo human gastrocnemius tendon. Journal of Biomechanics 2002;35(12):1639-1646.
43. Maganaris CN, Paul JP. Hysteresis measurements in intact human tendon. Journal of Biomechanics 2000;33(12):1723-1727.
44. Chu CC. Hydrolytic degradation of polyglycolic acid: Tensile strength and crystallinity study. Journal of Applied Polymer Science 1981;26(5):1727-1734.
45. Yuan X, Mak AFT, Yao K. Comparative observation of accelerated degradation of poly(-lactic acid) fibres in phosphate buffered saline and a dilute alkaline solution. Polymer Degradation and Stability 2002;75(1):45-53.
46. Nair LS, Laurencin CT. Biodegradable polymers as biomaterials. Progress in Polymer Science 2007;32(8-9):762-798.
47. Shearer H, Ellis MJ, Perera SP, Chaudhuri JB. Effects of common sterilization methods on the structure and properties of poly(D,L lactic-co-glycolic acid) scaffolds. Tissue engineering 2006;12(10):2717-2727.
48. Juncosa-Melvin N, Boivin GP, Galloway MT, Gooch C, West JR, Butler DL. Effects of cell-to-collagen ratio in stem cell-seeded constructs for Achilles tendon repair. Tissue engineering 2006;12(4):681-9.
49. Hoffmann A, Pelled G, Turgeman G, Eberle P, Zilberman Y, Shinar H, Keinan-Adamsky K, Winkel A, Shahab S, Navon G and others. Neotendon formation induced by manipulation of the Smad8 signalling pathway in mesenchymal stem cells. J. Clin. Invest 2006;116(4):940-952.

50. Altman G, Horan R, Martin I, Farhadi J, Stark P, Volloch V, Vunjak-Novakovic G, Richmond J, Kaplan DL. Cell differentiation by mechanical stress. The FASEB Journal 2002;16(2):270-272.

Figures

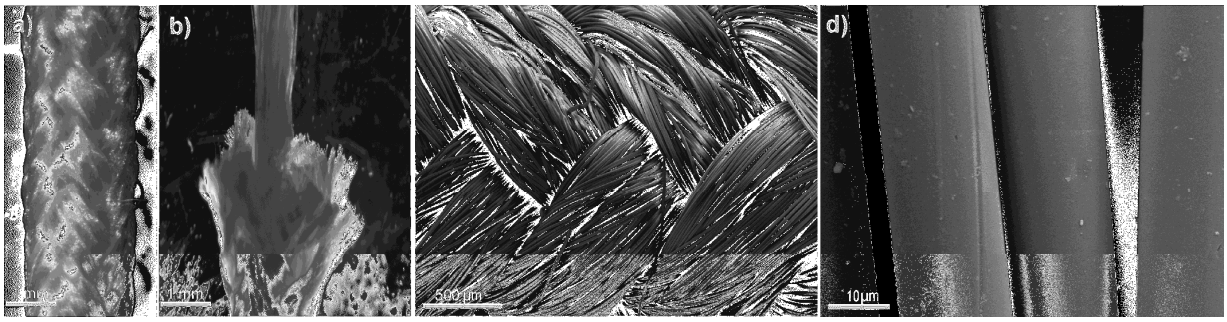

Figure 1. Morphology of the PLA braid, by optical (a and b) and electron microscopy (c and d). Overall macroscopic appearance (a), and detail to show the core thread around which the microfibers have been braided (b). Detail of the braiding angle (c) and of the single microfibers (d).

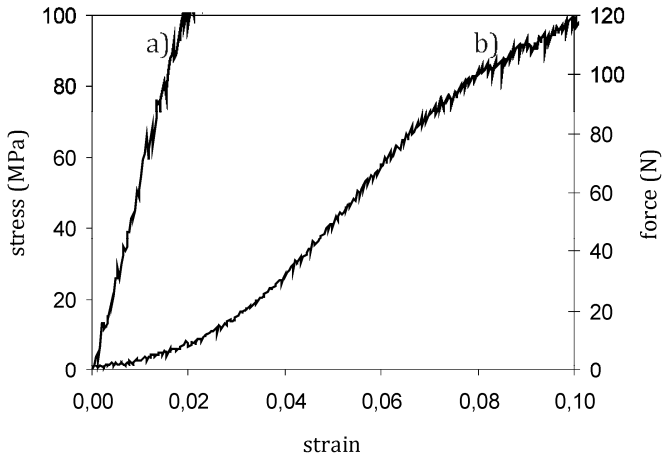

Figure 2. Typical stress (force) *versus* strain curves of four straight PLA threads (a) and of the PLA braid (b).

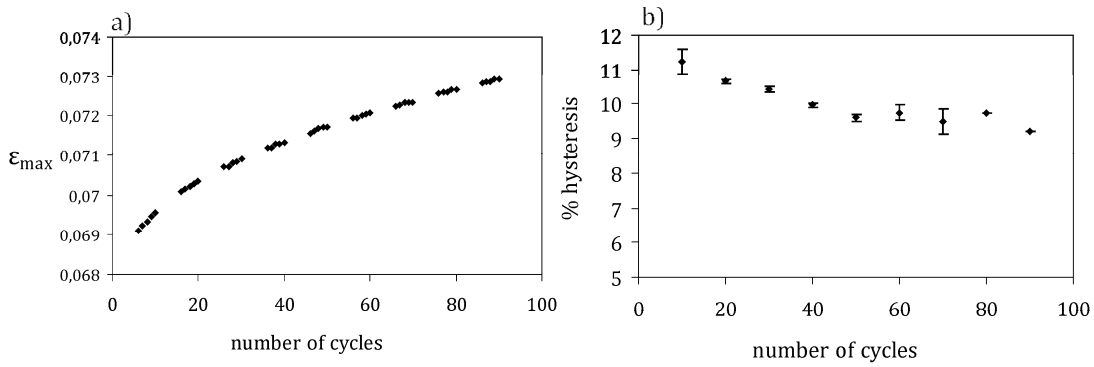

Figure 3. Mechanical properties of the PLA braid in dynamical tests. a) Increase of the maximal deformation with the number of cycles. b) Decrease of mechanical hysteresis with the number of cycles.

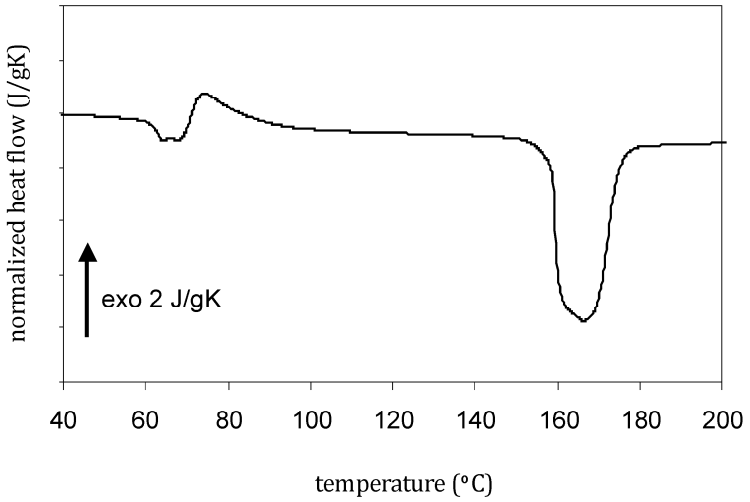

Figure 4. Normalized heat flow DSC thermogram of a PLA braid sample during a heating scan.

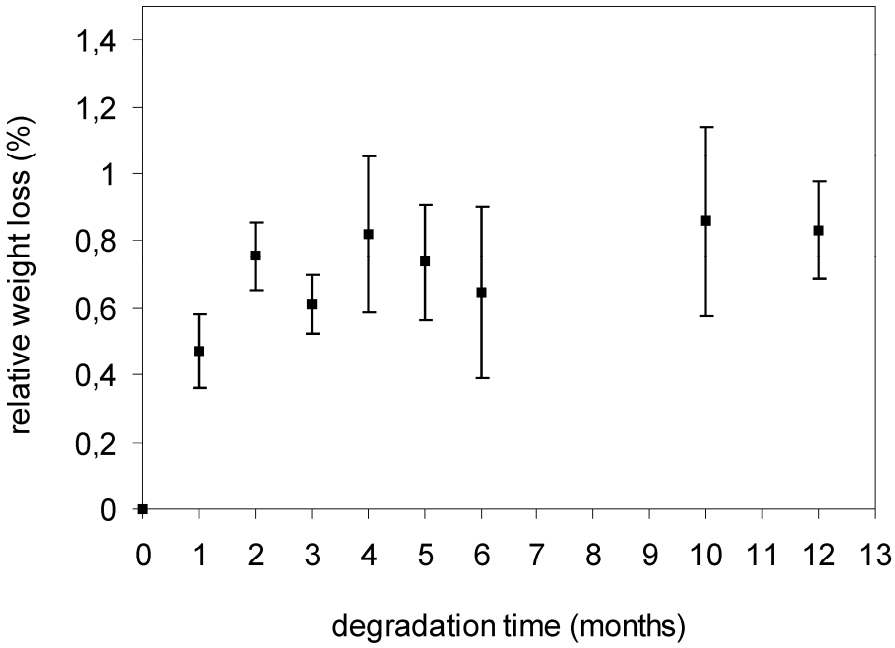

Figure 5. Relative weight loss of PLA braid during degradation tests *versus* degradation time.

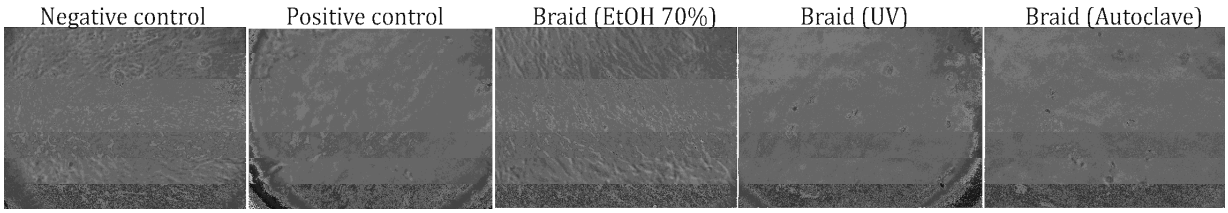

Figure 6. Optical microscopic images of L929 cells cultured with the supernatant of braids sterilized with different techniques after 7 days.

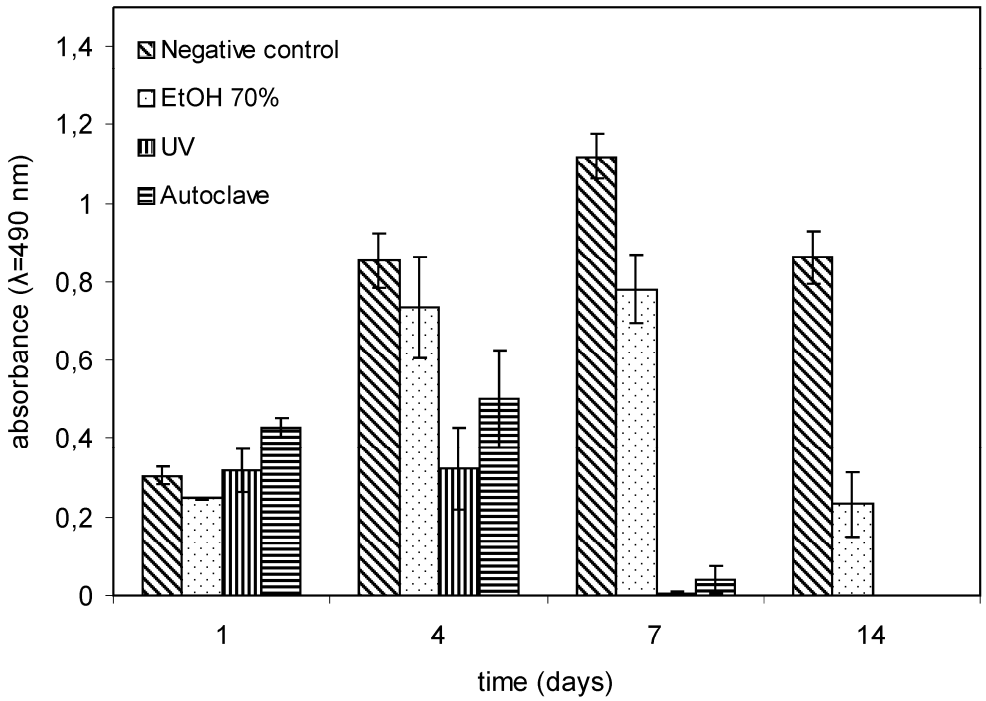

Figure 7. MTS assay on cells cultured with the supernatant of braids sterilized with different techniques (cytotoxicity assay, see text). Absorbance *versus* culture time.

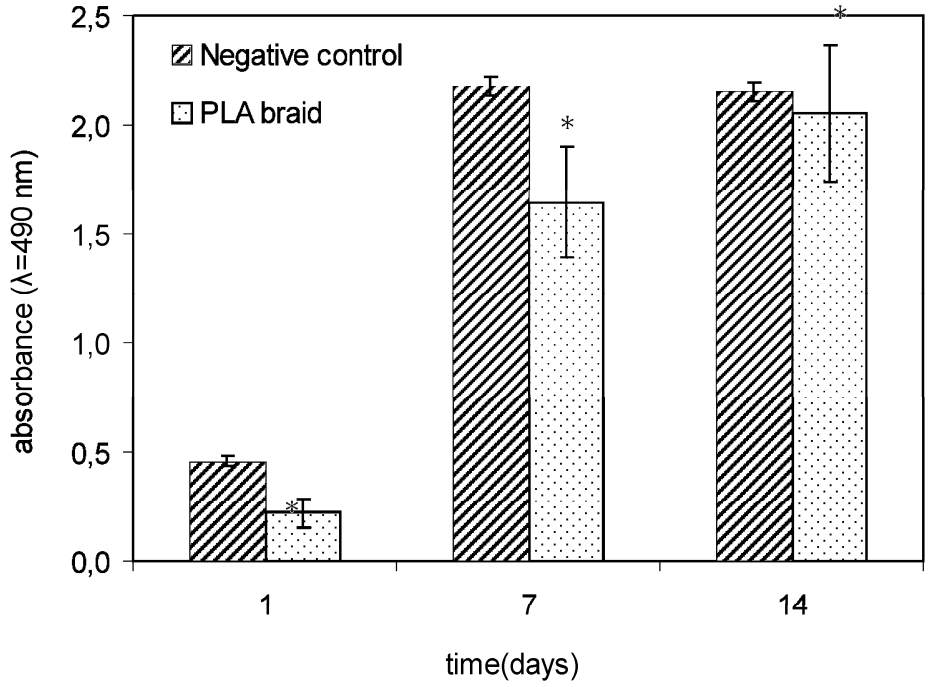

Figure 8. MTS assay for cell viability of fibroblasts cultured on braids. Absorbance *versus* culture time for 1, 7 and 14 culture days. (* $p < 0.05$).

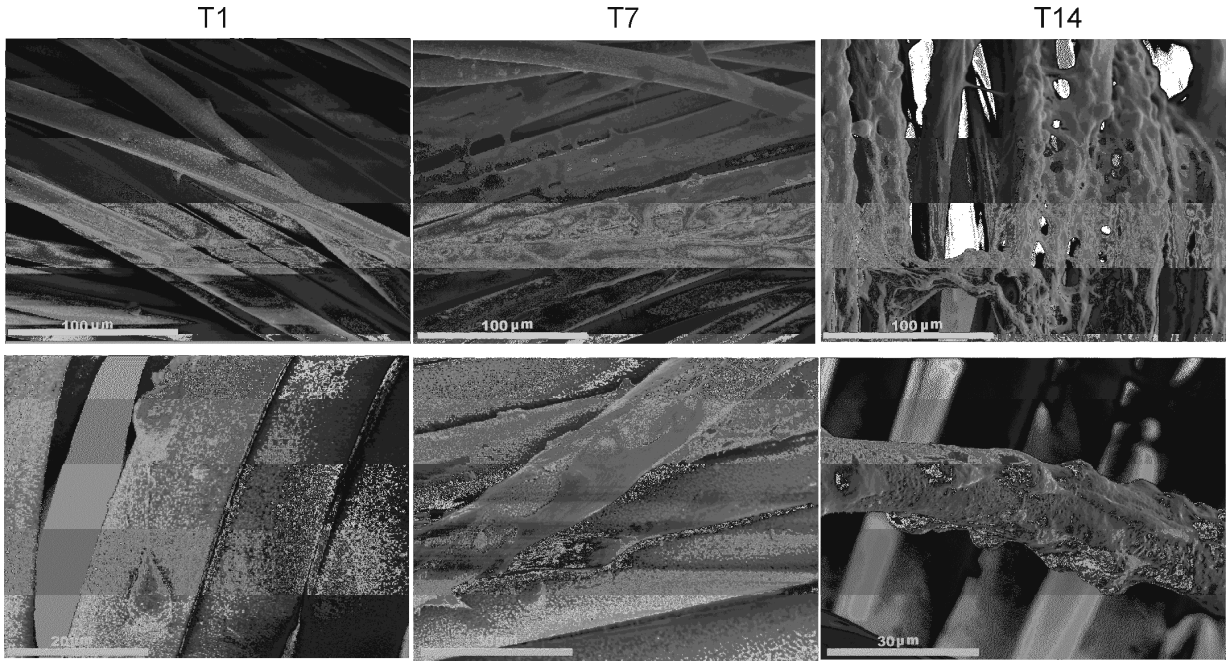

Figure 9. SEM micrographs of PLA braids seeded with L929 fibroblasts after 1, 7 and 14 culture days.

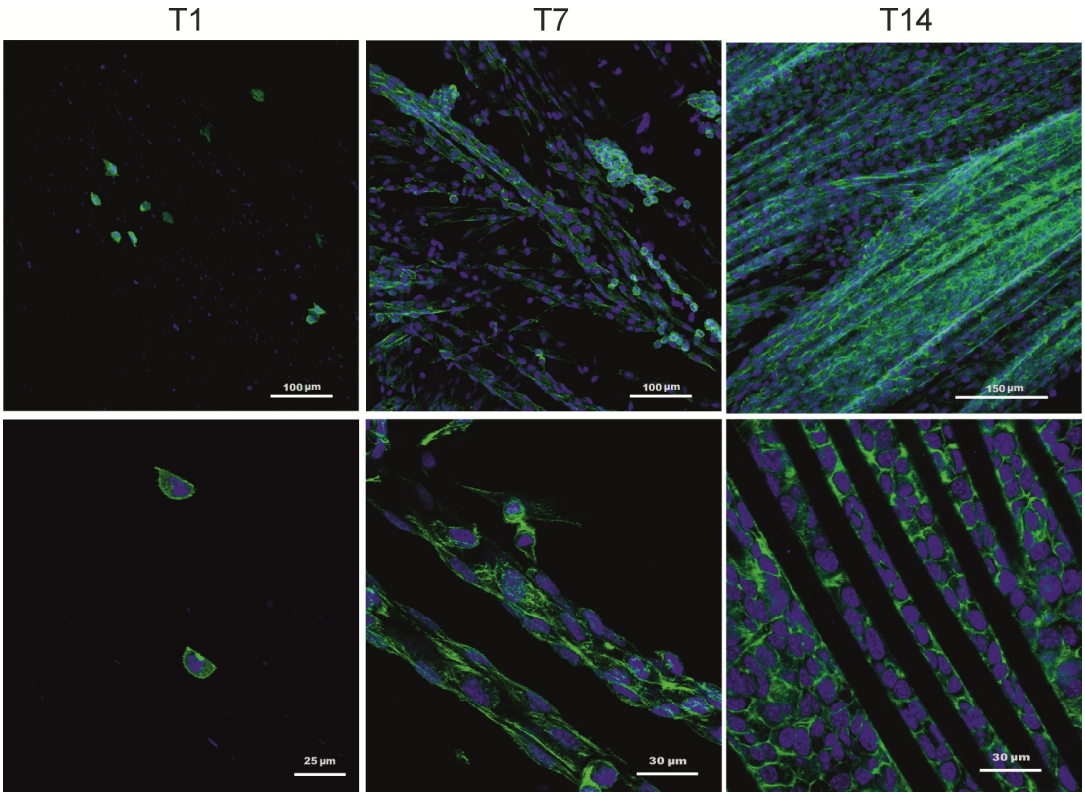

Figure 10. Fluorescence microscopy of L929 fibroblasts on PLA braids after 1, 7 and 14 culture days. Actin (cytoskeleton protein) seen in green (phallacidin stained), and cell nuclei in blue (DAPI stained).